Renormalization-group theory of an internal critical-end-point structure: The Blume-Emery-Griffiths model with biquadratic repulsion

Roland R. Netz
Institut für Festkörperforschung, Forschungszentrum Jülich, 5170 Jülich, Germany

A. Nihat Berker
Department of Physics, Massachusetts Institute of Technology, Cambridge, Massachusetts 02139
(Received 16 December 1992)

A prefaced renormalization-group study indicates that all three features of the Blume-Emery-Griffiths model with repulsive biquadratic interaction, namely (1) a critical-end-point structure occurring inside the ferromagnetic phase, (2) disordered-ferromagnetic-disordered reentrance, and (3) a ferrimagnetic phase sandwiched between the ferromagnetic and antiquadrupolar phases, survive fluctuations in three dimensions but not in two dimensions. The renormalization-group mechanism for a critical-end-point structure inside the ordered phase is shown to be the same as that originally found for a critical-end-point structure inside the disordered phase, namely a distinct hybrid fixed point, contrary to a previous claim.

I. INTRODUCTION

A recent study[1] of the global phase diagram of the Blume-Emery-Griffiths model[2] with repulsive biquadratic interaction, using mean-field theory, shows a variety of interesting features, including the following: at moderate repulsion, (1) a critical-end-point–critical-point structure occurring *inside* the ferromagnetically ordered phase, (2) *reentrance,* as temperature is lowered, with the phase sequence of disordered-ferromagnetic-disordered; and, at stronger repulsion, (3) a *ferrimagnetic* phase sandwiched between the ferromagnetic and antiquadrupolar phases. Of further interest are whether these features survive the fluctuations neglected in the mean-field theory and, if so, their dependence[3] on spatial dimensionality d. Thus, a more recent study[4] addressed these features using Monte Carlo renormalization-group theory and found that they indeed occur in $d=3$. The purpose of the current work is to address these questions without recourse to stochastic sampling and in different dimensions, using closed-form renormalization-group equations. The system was treated, in $d=2$ and 3, using an approximate position-space renormalization-group transformation, after a prefacing transformation.[5,6] We find that all three features occur in $d=3$, but not in $d=2$. Moreover, we find that the renormalization-group mechanism for the critical-end-point–critical-point structure occurring inside the ordered phase is the same as that originally found[7] for the critical-end-point–critical-point structure occurring inside the disordered phase, namely a hybrid fixed point, contrary to a previous claim.[8]

II. PREFACING TRANSFORMATION

A. The model

The Blume-Emery-Griffiths model[2] is a spin-1 Ising model, with most general up-down symmetric nearest-neighbor couplings, with Hamiltonian

$$-\beta\mathcal{H}_{\mathrm{BEG}}=\sum_{\langle ij\rangle}[Js_is_j+Ks_i^2s_j^2-\Delta(s_i^2+s_j^2)]\ , \tag{1}$$

where $s_i=\pm1,0$ at each site i of a d-dimensional lattice, and $\langle ij\rangle$ denotes summation over nearest-neighbor pairs of lattice sites. We are interested in repulsive biquadratic interaction, $K<0$. Due to ferromagnetic-antiferromagnetic symmetry in the lattices considered here, we take $J\geq0$ with no loss of generality.

B. Two dimensions

In $d=2$, we consider the square lattice and shall be referring to its two sublattices. In order to conserve the *possibility* of ferrimagnetic ordering, both dense and dilute local magnetizations must be projected in a renormalization-group transformation. The model is cast into a form that explicitly identifies these local degrees of freedom by using a prefacing transformation,[5,6]

$$\exp[-\beta\mathcal{H}_{\mathrm{RG}}(\{\phi_r\})]=\sum_{\{s_i\}}P(\{\phi_r\},\{s_i\})\exp[-\beta\mathcal{H}_{\mathrm{BEG}}(\{s_i\})]\ , \tag{2}$$

where $\phi_r=\pm S,\pm L$ is the local degree of freedom in each cell r, S and L representing dense and dilute, respectively. The crux of the prefacing transformation is in the projection matrix, $P(\{\phi_r\},\{s_i\})$, which is factored over cells in the original lattice,

$$P(\{\phi_r\},\{s_i\})=\prod_r p(\phi_r,\{s_j\}_r)\ , \tag{3}$$

where $\{s_j\}_r$ are the spins in cell r. We use the simplest possible cells, which are squares that contain four nearest-neighbor spins. On neighboring cells, spins on alternate sublattices affect the projection operator:

 ©1993 The American Physical Society

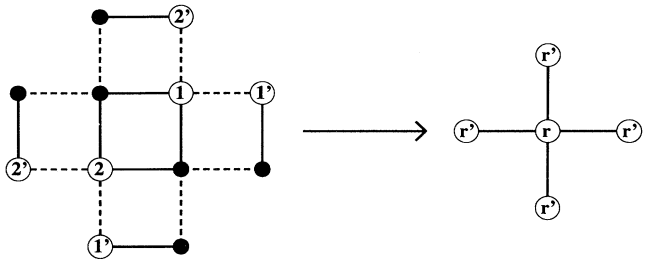

FIG. 1. Finite cluster of two square cells, with periodic boundary conditions, used in the prefacing transformation in two dimensions. The sites affecting the projection operator are numbered. On the left, dashed and full lines respectively correspond to intercell and intracell bonds.

$$p(\phi,s_1,s_2)=\tfrac{1}{2}[1+\mathrm{sgn}(\phi)\mathrm{sgn}(s_1+s_2)]D(|\phi|,s_1^2+s_2^2)\ , \tag{4}$$

where the signum function is $\mathrm{sgn}(x)=\pm 1$ or 0 for $x\gtrless 0$ or 0, respectively, and s_1 and s_2 are the two spins on the same sublattice. The density projection operator is taken as

$$\begin{aligned} &D(|\phi|,2)=1,0\ , \\ &D(|\phi|,1)=\alpha,1-\alpha\ , \\ &D(|\phi|,0)=0,1\ , \end{aligned} \tag{5}$$

for $|\phi|=S,L$, respectively, and $\alpha=\frac{1}{8}$ is taken so as to give equal weight to each state of the prefaced system. Finally, the summation in Eq. (2) is effected approximately using a finite system of two cells with periodic boundary conditions, as shown in Fig. 1.

C. Three dimensions

In $d=3$, we consider the cubic lattice and shall be referring also to its two sublattices. Analogous procedures in $d=3$ and 2 are chosen, in order to validate comparisons between results. For the prefacing transformation, we use the simplest possible cells, which are cubes that contain eight nearest-neighbor spins. On neighboring cells, spins on alternate sublattices affect the projection operator. The cell projection operator is taken as the arithmetic average of the cell projection operator in Sec. II B applied to each pair of nearest-neighbor spins on the same sublattice in the cell. The summation of Eq. (2) is effected approximately, using a finite system of two cells with periodic boundary conditions, as shown in Fig. 2.

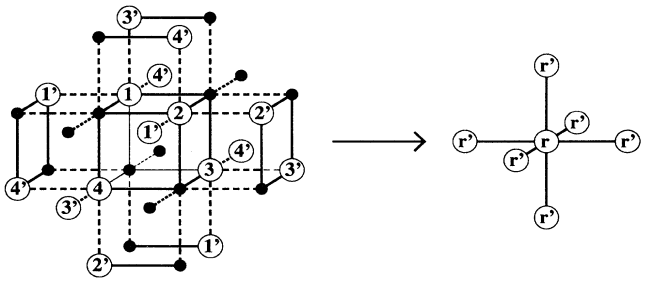

FIG. 2. Finite cluster of two cubic cells, with periodic boundary conditions, used in the prefacing transformation in three dimensions. The sites affecting the projection operator are numbered. On the left, dashed and full lines respectively correspond to intercell and intracell bonds.

III. RESULTS

A. Renormalization-group sinks

The prefaced models are solved using the Migdal-Kadanoff renormalization-group approximation,[9,10] consisting of bond moving followed by decimation with a length rescaling factor of $b=3$. Alternatively, our results constitute exact solutions of the prefaced model on hierarchical lattices[11] with $d=2$ and 3.

Under renormalization-group iterations, each point of a thermodynamic phase, specified by initial (J,K,Δ), maps onto a "sink" that epitomizes that thermodynamic phase.[7] The sinks occurring in this study, corresponding to the dense ferromagnetic, dilute ferromagnetic, ferrimagnetic, and antiquadrupolar ordered phases, and the dense and dilute disordered phases, are given in Fig. 3 via their transfer matrices. Note that the ferrimagnetic and antiquadrupolar phases are determined by the off-diagonal elements of the corresponding sink transfer matrix exhibited in Fig. 3. Examination of this figure shows that we have prefaced onto the minimal model for the study of the three different types of order here.

B. Phase diagrams in two and three dimensions

Representative phase diagram cross sections for repulsive biquadratic couplings are shown in Fig. 4, for $d=2$ and 3.

For $d=2$, for moderately repulsive biquadratic couplings such as $K/J=-0.5$ [Fig. 4(a)], there occurs a tri-

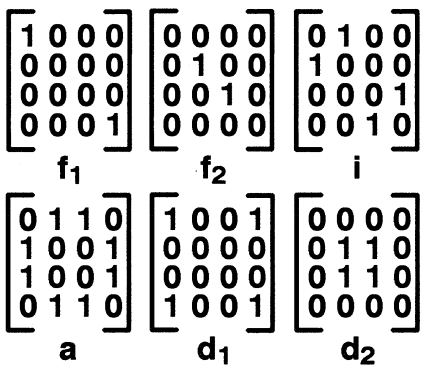

FIG. 3. Values of the nearest-neighbor transfer matrix $\exp[-\beta\mathcal{H}(\phi_{r'},\phi_r)]$ at the renormalization-group sinks: dense ferromagnetic (f_1), dilute ferromagnetic (f_2), ferrimagnetic (i), antiquadrupolar (a), dense disordered (d_1), and dilute disordered (d_2).

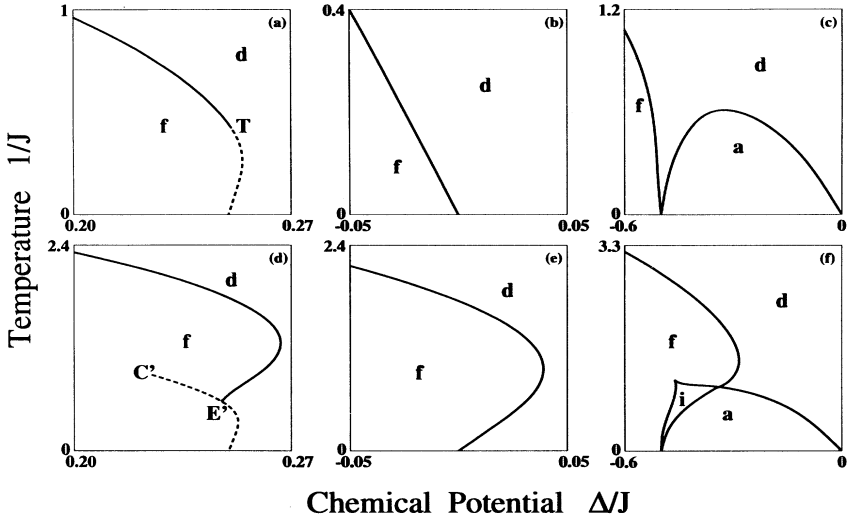

FIG. 4. Calculated phase diagrams: (a) $d=2$, $K/J=-0.5$; (b) $d=2$, $K/J=-1$; (c) $d=2$, $K/J=-1.5$; (d) $d=3$, $K/J=-0.5$; (e) $d=3$, $K/J=-1$; (f) $d=3$, $K/J=-1.5$. The ferromagnetic (*f*), ferrimagnetic (*i*), antiquadrupolar (*a*), and disordered (*d*) phases are marked. Dashed and full curves respectively correspond to first- and second-order phase boundaries.

critical phase diagram with reentrant structure, exhibiting disordered-ferromagnetic-disordered phases as temperature $1/J$ is lowered at constant chemical potential Δ/J. However, this reentrance is less pronounced than in $d=3$ (see below). As K/J is made more negative, the first-order transitions and the reentrant behavior both disappear to yield the sole, nonreentrant critical line at $K/J=-1$ [Fig. 4(b)]. For more repulsive biquadratic couplings such as $K/J=-1.5$ [Fig. 4(c)], an antiquadrupolar phase appears and is separated from the ferromagnetic phase by the disordered phase that extends to a zero-temperature disorder point. This sequence is very similar to results from an unprefaced Migdal-Kadanoff renormalization-group study[3] for $d=2$.

Qualitatively different behavior occurs in $d=3$. For moderately repulsive biquadratic coupling $K/J=-0.5$ [Fig. 4(d)], a critical-end-point (E')–isolated-critical-point (C') structure occurs inside the ordered (ferromagnetic) phase. This structure had been, in general, previously seen in classical theories,[12–14,1] but not in a renormalization-group theory. The corresponding mechanism will be described in Sec. III C below. At $K/J=-1$ [Fig. 4(e)], the first-order transitions disappear, but the reentrance persists. For more repulsive biquadratic coupling, $K/J=-1.5$ [Fig. 4(f)], a ferrimagnetic phase occurs. It is bounded by the ferromagnetic and antiquadrupolar phases. The three different ordered phases meet at a single finite-temperature point. (The unprefaced study[3] did indicate a qualitative dimensionality dependence of the phase diagrams, but the lack of renormalization-group flow space excluded the possibility of the new sinks occurring here.) Reentrance and, possibly,[12,13,15] critical-end-point structure, as above, has been seen[16,17] in the analogous experimental system of $FeBr_2$.

Due to the approximate nature of the calculation, we cannot trust the detailed description of the phase boundaries obtained. However, looking at the broad features of the phase diagrams, the novel features seen in mean-field theory appear to survive the fluctuations in $d=3$, but not in $d=2$.

C. Internal and external critical-end-point structures in renormalization-group theory

Renormalization-group theory was invented[18] in 1971 to describe critical behavior. First-order behavior was

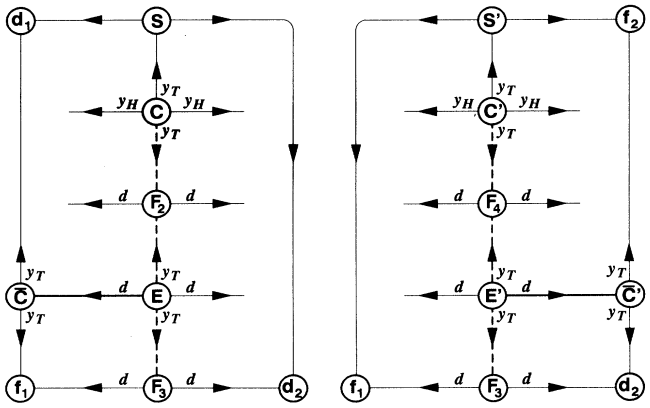

FIG. 5. Renormalization-group mechanism for critical end points with the first-order segment occurring: (left panel) inside the disordered phase, found in Ref. 7 ("external" structure); (right panel) inside the ordered phase, found in this work ("internal" structure). In both cases, the mechanism involves a distinct, hybrid fixed point (E and E') onto which the critical end points renormalize. The fixed-point connectivity and relevant eigenvalue exponents are shown, including the $y=d$. The critical eigenvalue exponents y_T and y_H appear numerically identically at distinct fixed points within each connectivity. Trajectories coinciding with first- or second-order phase boundaries are drawn as dashed or thick lines, respectively. The phase sinks, represented by the circled lower-case letters, are identified in Fig. 3. The unstable fixed points S and S' are no-transition fixed points, combining, in their transfer matrix, the unit elements of the sinks they mediate and, additionally, all corresponding off-diagonal elements at unit value (i.e., no coupling). The subscript n of the first-order fixed points F_n indicates the number of coexisting phases.

TABLE I. Location and eigenvalue exponents of the fixed point (E' in Fig. 5) of the critical end point [E' in Fig. 4(d)] and of the fixed point ($\bar{C}'$ in Fig. 5) of the critical line leading into the end point ($d=3$).

Critical end point (E')	Critical line (leading into E')
Fixed-point location in terms of nearest-neighbor transfer matrix $\exp[-\beta\mathcal{H}(\phi_{r'},\phi_r)]$	
$\begin{bmatrix} 1 & 0 & 0 & 0 \\ 0 & u & v & 0 \\ 0 & v & u & 0 \\ 0 & 0 & 0 & 1 \end{bmatrix}$	$\begin{bmatrix} 0 & 0 & 0 & 0 \\ 0 & u & v & 0 \\ 0 & v & u & 0 \\ 0 & 0 & 0 & 0 \end{bmatrix}$
with $u=0.979$, $v=0.905$.	
Note that these two matrices are *globally separated* in renormalization-group flow space.	
Leading eigenvalue exponents	
$y_1=3=d$, $y_2=0.925$	$y_1=0.925$, $y_2=-8.2$

discerned[19] in renormalization-group theory in 1975. Critical-end-point behavior was discerned,[7] in renormalization-group theory, shortly thereafter.

The first critical end points seen in renormalization-group theory had the first-order segment, connecting the end point and the isolated critical point, occur inside the disordered phase (we shall call this structure "external"). From that work,[7] the end-point mechanism in renormalization-group theory was revealed as a distinct critical-end-point fixed point that exhibits both the relevant eigenvalue exponents of the critical fixed point and the eigenvalue exponent $y=d$ of the first-order fixed point (Fig. 5). Thus, the critical-end-point fixed point was called a hybrid fixed point. Nevertheless, a subsequent work[8] claimed that critical end points with the first-order segment occurring inside the ordered phase (which we shall call an "internal" structure) did not derive, in renormalization-group theory, from this mechanism of a distinct, hybrid fixed point. However, we find here that the latter claim is incorrect: Table I lists the location and eigenvalue exponents of the distinct fixed point of the critical end point in the current work (which has the internal structure) and those of the fixed point of the critical line leading into the critical end point. It is seen that we have again a hybrid fixed point. Thus, the renormalization-group mechanism for "internal" critical-end-point structures is identical with the one originally seen for "external" critical-end-point structures.

ACKNOWLEDGMENTS

We thank W. Hoston for useful discussions. This research was supported by NSF Grant No. DMR-90-22933 and JSEP Contract No. DAAL 03-92-C0001.

[1]W. Hoston and A. N. Berker, Phys. Rev. Lett. **67**, 1027 (1991).
[2]M. Blume, V. J. Emery, and R. B. Griffiths, Phys. Rev. A **4**, 1071 (1971).
[3]W. Hoston and A. N. Berker, J. Appl. Phys. **70**, 6101 (1991).
[4]R. R. Netz, Europhys. Lett. **17**, 373 (1992).
[5]A. N. Berker, Phys. Rev. B **12**, 2752 (1975).
[6]A. N. Berker, S. Ostlund, and F. A. Putnam, Phys. Rev. B **17**, 3650 (1978).
[7]A. N. Berker and M. Wortis, Phys. Rev. B **14**, 4946 (1976).
[8]T. A. L. Ziman, D. J. Amit, G. Grinstein, and C. Jayaprakash, Phys. Rev. B **25**, 319 (1982).
[9]A. A. Migdal, Zh. Eksp. Teor. Fiz. **69**, 1457 (1975) [Sov. Phys. JETP **42**, 743 (1976)].
[10]L. P. Kadanoff, Ann. Phys. (N.Y.) **100**, 359 (1976).
[11]A. N. Berker and S. Ostlund, J. Phys. C **12**, 4961 (1979).
[12]J. M. Kincaid and E. G. D. Cohen, Phys. Lett. **50A**, 317 (1974).
[13]J. M. Kincaid and E. G. D. Cohen, Phys. Rep. C **22**, 57 (1975).
[14]P. H. E. Meijer and W. C. Stamm, Physica A **90**, 77 (1978).
[15]E. Stryjewski and N. Giordano, Adv. Phys. **26**, 487 (1977).
[16]A. R. Fert, P. Carrara, M. C. Lanusse, G. Mischler, and J. P. Redoules, J. Phys. Chem. Solids **34**, 223 (1973).
[17]C. Vettier, H. L. Alberts, and D. Bloch, Phys. Rev. Lett. **31**, 1414 (1973).
[18]K. G. Wilson, Phys. Rev. B **4**, 3174, 3184 (1971).
[19]B. Nienhuis and M. Nauenberg, Phys. Rev. Lett. **35**, 477 (1975).